Journal of Microelectronics and Electronic Packaging (2014) **11**, 181-196

ISSN: 1551-4897

Causality Verification Using Polynomial Periodic Continuations for Electrical Interconnects

Lyudmyla L. Barannyk,[1,*] Hazem A. Aboutaleb,[2,3] Aicha Elshabini,[2] and Fred Barlow[2]

***Abstract*—We present a method for checking causality of band-limited tabulated frequency responses. The approach is based on Kramers-Krönig relations and construction of periodic polynomial continuations. Kramers-Krönig relations, also known as dispersion relations, represent the fact that real and imaginary parts of a causal function form a Hilbert transform pair. The Hilbert transform is defined on an infinite domain, while, in practice, discrete values of transfer functions that represent high-speed interconnects are available only on a finite frequency interval. Truncating the computational domain or approximating the behavior of the transfer function at infinity causes significant errors at the boundary of the given frequency band. The proposed approach constructs a periodic polynomial continuation of the transfer function that is defined by raw frequency responses on the original frequency interval and by a polynomial in the extended domain, and requires the continuation to be periodic on a wider domain of a finite length and smooth at the boundary. The dispersion relations are computed spectrally using fast Fourier transform and inverse fast Fourier transform routines applied to periodic continuations. The technique does not require the knowledge or approximation of the transfer function behavior at infinity. The method significantly reduces the boundary artifacts that are due to the lack of out-of-band frequency responses, and is capable of detecting small, smooth causality violations. We perform the error analysis of the method and show that its accuracy and sensitivity depend on the smoothness and accuracy of data and a polynomial continuation. The method can be used to verify and enforce causality before the frequency responses are employed for macromodeling. The performance of the method is tested on several analytic and simulated examples.**

***Keywords*—Causality, dispersion relations, periodic continuation, periodic polynomial continuation, Hilbert transform, fast Fourier transform, FFT, causality violations**

Introduction

Electrical interconnects are an important part of high-speed digital systems. They need to be designed properly to provide correct system performance and avoid signal and power integrity problems, which requires systematic simulations of suitable models at different levels [1]. These models should be able to capture the relevant electromagnetic phenomena. The models are constructed using the results of direct measurements or full-wave electromagnetic simulations. The data are in the form of discrete port frequency responses and they represent scattering, impedance, or admittance transfer matrices or transfer functions, depending on whether multi-dimensional or scalar cases are considered. The frequency responses are then employed to derive a macromodel. Several techniques can be used to accomplish this, including the vector fitting [2], the orthonormal vector fitting [3], and others. However, the data are often contaminated by errors that come from a noise or inadequate calibration, in the case of direct measurements, or approximation and discretization errors arising in numerical simulations. In addition, the frequency responses are usually available over a finite frequency range in a discrete form with a limited number of samples. All this may affect the performance of the macromodeling technique, resulting in nonconvergence of the algorithm or inaccurate models. Using such models in subsequent time-domain simulations may lead to flawed results or software failure, even when advanced electromagnetic solvers are employed. Often the underlying cause of such problems is the lack of causality in raw frequency response data [4].

Causality of a physical system can be defined in both time and frequency domains. The time domain definition states that a system is causal if the effect always follows the cause. For linear time-invariant systems with the impulse response h, this implies that $h(t) = 0$ for $t < 0$. Having a nonzero value of $h(t)$ for some $t < 0$ indicates a causality violation. To verify causality using this definition, one can convert frequency responses from the frequency domain to the time domain, using an inverse discrete Fourier transform. This approach suffers from the well-known Gibbs phenomenon, since the frequency responses represent Fourier transform of impulse response functions that are typically nonsmooth because of the presence of delayed reflections. Having frequency responses on a finite interval results in a truncation of slowly decaying Fourier series, which causes severe overshooting and undershooting near the singularities, such as jump discontinuities, of impulse response functions and their derivatives. The problem of slow decay of the Fourier spectrum is usually addressed by windowing the Fourier data [5, Ch. 7]. There are other filtering techniques that deal with the Gibbs phenomenon by taking into account information about singularities [6-8]. In a related paper [9], a nonlinear extrapolation of Fourier data is employed to avoid the Gibbs phenomenon and the use of windows/filtering.

The manuscript was received on June 18, 2014; revision received on September 23, 2014; accepted on September 24, 2014.

[1]Department of Mathematics, University of Idaho, Moscow, Idaho
[2]Department of Electrical & Computer Engineering, University of Idaho, Moscow, Idaho
[3]The Egyptian Armed Forces, Cairo, Egypt
*Corresponding author; email: barannyk@uidaho.edu

doi:10.4071/imaps.428

In the frequency domain, causality is defined in terms of the transfer function $H(w)$ that is the Fourier transform of the time-domain impulse response function $h(t)$. A system is said to be causal if $H(w)$ satisfies dispersion relations also known as Kramers-Krönig relations [10, 11]. Dispersion relations can be written in terms of the Hilbert transform, and state the real and imaginary parts of a causal function form a Hilbert transform pair. The dispersion relations are extremely important in many areas of physics, science and engineering. In particular, in electronics, they are used in reconstruction [12] and correction [13, 14] of measured data; delay extraction [15-17]; time-domain conversion [18]; estimation of optimal bandwidth and data density [19]; and various causality verification and enforcement techniques that are based on minimum phase and all-pass decomposition [16, 17, 20-22], generalized dispersion relations with subtractions [23-25], causality characterization via analytic continuation for L_2 integrable functions [26], and causality enforcement using periodic continuations [27, 28], which is the subject of the current study.

To characterize causality in the frequency domain using dispersion relations, one needs to deal with the Hilbert transform that is defined on the infinite domain. The integration can be reduced to $[0, \infty]$ by symmetry of $H(w)$ for real-valued impulse response functions h. However, in practice, the values of $H(w)$ are usually available over a finite-length frequency interval as a discrete set of frequency responses. Therefore, domain of integration needs to be either truncated or the behavior of $H(w)$ for large w needs to be approximated. This is inevitable, since measurements can only be practically conducted over a finite frequency range. Similarly, a computational domain needs to be finite and its size should be limited to control simulation cost. One of the approaches to deal with these problems is to assume that $H(w)$ is square integrable, since this would imply that $H(w)$ tends to zero at infinity, which would allow domain truncation or enable extrapolation/continuation of data to infinity. If, instead, $H(w)$ does not decay at infinity and remains bounded or even grows as w increases, the generalized dispersion relations with subtractions can be used to decrease the sensitivity of data at high frequencies and allow domain truncation [23-25]. For review of some previous work done to address the problem of having data on a bandlimited interval, please see [25].

We present an alternative approach that deals with bandlimited data, not periodic in general, by constructing a polynomial periodic continuation and requiring the transfer function to be periodic on a wider domain of finite length. Then we use dispersion relations of periodically continued data to verify causality on the original frequency interval and enforce it if necessary. The dispersion relations are computed in a convolution form using spectrally accurate fast Fourier transform (FFT) routine and its inverse (IFFT) that are designed for periodic functions [29]. The preliminary results were reported in [27], where the periodic continuations were applied to general transfer functions $H(w)$, for which the impulse response functions $h(t)$ are not necessarily real.

In this paper, we consider the case when $h(t)$ is real. Then the real and imaginary parts of $H(w)$ are even and odd functions, respectively, which gives symmetry conditions on the frequency response data. It is known that direct application of FFT/IFFT to nonperiodic data results in boundary artifacts. We demonstrate that the proposed method is capable of decreasing such boundary errors and its accuracy primarily depends on the degree of a polynomial or smoothness of the continuation. The method is capable of detecting smooth causality violations that are typically difficult to detect [25]. We perform the error analysis of the method in the presence of a noise or approximation errors in the data, and show that this error depends on the smoothness and accuracy of the given frequency responses, as well as smoothness and accuracy of a periodic continuation in the extended domain.

The paper is organized as follows. We provide background on causality of linear time-invariant systems, dispersion relations, and motivation for the proposed method. Then we present a periodic polynomial continuation method and develop the error estimates for this method. The performance of the proposed technique is demonstrated on several analytic and simulated examples, both causal and noncausal. Finally, we provide our conclusions.

Causality and Dispersion Relations

Causality is a fundamental physical property and it is valid in all areas of physics. Consider a scalar system with an impulse response function $h(t,t')$ and an input $f(t)$ to which it responds with an output $x(t)$. If the output $x(t)$ is a linear function of the input $f(t)$ and the impulse response h is time-invariant, then the response $x(t)$ can be written as a convolution of the input $f(t)$ and the impulse response $h(t - t')$ [30]:

$$x(t) = \int_{-\infty}^{\infty} h(t - t')f(t')dt' = h(t) * f(t). \tag{1}$$

The Fourier transform F of the impulse response function h, denoted by $H(w)$, is called the transfer function and it is

$$\mathrm{F}[h](w) = \int_{-\infty}^{\infty} h(\tau)\mathrm{e}^{-iw\tau}d\tau \equiv H(w). \tag{2}$$

Please note that we use an opposite sign in the definition of the Fourier transform than in [30]. For a multicomponent system, the transfer function generalizes to the transfer matrix. In this work, we restrict ourselves to a scalar case. The approach can be generalized to multicomponent cases by considering each entry of the transfer matrix separately.

The primitive causality principle, stated in the time domain, says that no output $x(t)$ can occur before the input $f(t)$ or, in other words, no effect can precede its cause. This implies that if $f(t) = 0$ for $t < T$, then the same is true for $x(t)$. As a consequence, the impulse response function has to satisfy the condition

$$h(\tau) = 0, \quad \tau < 0, \tag{3}$$

and the transfer function in eq. (2) becomes

$$H(w) = \int_{0}^{\infty} h(\tau)\mathrm{e}^{-iw\tau}d\tau. \tag{4}$$

Since the integral in (4) is extended only over a half-axis, function $H(w)$ has a regular analytic continuation in the lower half w-plane.

Physical systems that satisfy these conditions include common network representations, such as scattering, with f and x being power waves; impedance, with f being currents and x, voltages; and admittance, with f being voltages and x being currents.

If we assume that h is a square integrable function, that is, $h \in L^2(R^+)$, then $H(w) \in L^2(R)$ by the Paley-Wiener theorem [31] (H is actually analytic in the lower half plane, square integrable, and it is called a Hardy function, $H(w) \in H^2(R)$). The converse also holds [30, 26]. Moreover, the real and imaginary parts of Hardy functions are not independent of each other. Let $H(w) = \mathrm{R}eH(w) + i\mathrm{I}mH(w)$. Starting from Cauchy integral representation for analytic functions and applying a limiting procedure as w tends to the real axis from below, one obtains that $H(w)$ satisfies the following integral identities:

$$\mathrm{R}eH(w) = \frac{1}{\pi} PV \int_{-\infty}^{\infty} \frac{\mathrm{I}mH(w')}{w - w'} dw', \tag{5}$$

$$\mathrm{I}mH(w) = -\frac{1}{\pi} PV \int_{-\infty}^{\infty} \frac{\mathrm{R}eH(w')}{w - w'} dw', \tag{6}$$

where

$$PV \int_{-\infty}^{\infty} = \lim_{\varepsilon \to 0} \left(\int_{-\infty}^{w-\varepsilon} + \int_{w+\varepsilon}^{\infty} \right)$$

denotes Cauchy's principal value. Eqs. (5) and (6) are called dispersion relations or Kramers-Krönig relations. They were originally formulated for problems of light propagation in a dispersive medium [10,11]. Dispersion relations are the frequency-domain counterpart of the causality condition. They show that given either ReH or ImH as an arbitrary square integrable function, another can be determined or reconstructed by causality. In mathematics, Kramers-Krönig relations are also called a Hilbert transform pair. Recall that the Hilbert transform is defined by

$$\mathrm{H}[u(w)] = \frac{1}{\pi} PV \int_{-\infty}^{\infty} \frac{u(w')}{w - w'} dw'.$$

Then dispersion relations can be written as

$$\mathrm{R}eH(w) = \mathrm{H}[\mathrm{I}mH(w)], \quad \mathrm{I}mH(w) = -\mathrm{H}[\mathrm{R}eH(w)],$$

i.e. ReH and ImH are Hilbert transforms of each other.

If the time-domain impulse response function $h(t)$ is real-valued, then R$eH(w)$ and I$mH(w)$ are even and odd functions, respectively. Using these symmetries in (5), (6) produces

$$\mathrm{R}eH(w) = \frac{2}{\pi} PV \int_0^{\infty} \frac{w' \mathrm{I}mH(w')}{w^2 - (w')^2} dw' \tag{7}$$

$$\mathrm{I}mH(w) = \frac{2w}{\pi} PV \int_0^{\infty} \frac{\mathrm{R}eH(w')}{w^2 - (w')^2} dw'. \tag{8}$$

Practical application of dispersion relations (5), (6) or (7), (8) poses some difficulties. The transfer function $H(w)$ is usually available only at a discrete set of frequencies over a finite bandwidth $[w_{min}, w_{max}]$, with $w_{min} \geq 0$, while the range of integration in (7), (8), for example, extends from zero to infinity. Dispersion relations require numerical evaluation of the singular integrals, but the bandwidth may not be sufficiently wide for convergence. Moreover, in some cases, $H(w)$ may not be square integrable at all and may only be bounded or behave as $O(w^n)$, when $|w| \to \infty$, $n = 0, 1, 2, \ldots$. Direct application of dispersion relations (7), (8) may result in a large truncation error in boundary regions of the given frequency interval $[w_{min}, w_{max}]$, producing significant boundary artifacts. The generalized dispersion relations with subtractions [32, 30] can be used to increase the convergence of the dispersion integrals by making integrands less sensitive to the high-frequency behavior, and, thus, reduce the reconstruction errors caused by the finite bandwidth. This approach has been used in [23-25] to develop a causality verification tool for bandlimited tabulated frequency responses. A recent paper [14] employes the dispersion relations with subtractions to improve accuracy of vector network analyzer, scattering parameter device characterization.

In general, for a decaying at infinity impulse response function $h(t)$, the asymptotic behavior of its Fourier transform $H(w)$ may approach a constant H_∞ as $|w| \to \infty$. This implies that the impulse response function $h(t)$ has a delta function present at $t = 0$. For impulse response functions that do not contain such singularities, $H_\infty = 0$. Writing $H_\infty = R_\infty + iI_\infty$, the dispersion relations (5), (6) become [13]

$$\mathrm{R}eH(w) = \frac{1}{\pi} PV \int_{-\infty}^{\infty} \frac{\mathrm{I}mH(w')}{w - w'} dw' + R_\infty, \tag{9}$$

$$\mathrm{I}mH(w) = -\frac{1}{\pi} PV \int_{-\infty}^{\infty} \frac{\mathrm{R}eH(w')}{w - w'} dw' + I_\infty. \tag{10}$$

Because of the odd symmetry of ImH and its uniqueness, $I_\infty = 0$. Hence, eq. (10) reduces to

$$\mathrm{I}mH(w) = -\frac{1}{\pi} PV \int_{-\infty}^{\infty} \frac{\mathrm{R}eH(w')}{w - w'} dw'. \tag{11}$$

Generalized dispersion relations (9), (11) imply that ImH can be determined from ReH, while ReH is determined from ImH to within a constant. This suggests that when it is not known that $H(w)$ decays to zero as $|w| \to \infty$, causality can be verified by reconstructing ImH from ReH and comparing the result with the given ImH, while reconstructing ReH from ImH would require the knowledge of R_∞. For this reason, in what follows we will employ ReH to reconstruct ImH.

Using convolution operation we can write (9), (11) as

$$\mathrm{R}eH(w) = \frac{1}{\pi w} * \mathrm{I}mH(w) + R_\infty, \tag{12}$$

$$\mathrm{I}mH(w) = -\frac{1}{\pi w} * \mathrm{R}eH(w). \tag{13}$$

Convolution can be computed using Fourier transform F and its inverse F^{-1} via convolution theorem to give

$$\mathrm{R}eH(w) = \mathrm{F}^{-1}\left[\mathrm{F}\left[\frac{1}{\pi w} \right] \cdot \mathrm{F}[\mathrm{I}mH(w)] \right] + R_\infty, \tag{14}$$

$$\mathrm{I}mH(w) = -\mathrm{F}^{-1}\left[\mathrm{F}\left[\frac{1}{\pi w} \right] \cdot \mathrm{F}[\mathrm{R}eH(w)] \right]. \tag{15}$$

The Fourier transform of $\frac{1}{\pi w}$ is evaluated using the contour integration [33, p.240-242]

$$\mathrm{F}\left[\frac{1}{\pi w}\right] = PV\int_{-\infty}^{\infty}\frac{e^{-ikw}}{\pi w}dw = i\,sgn(k), \tag{16}$$

where k is the wave number. Eqs. (14), (15) provide a way of reconstructing ImH from ReH and vice versa. Discrete Fourier transform and its inverse can be computed employing FFT/IFFT subroutines. However, these techniques are designed for periodic functions, while the transfer functions $H(w)$ are not periodic in general. Direct application of FFT/IFFT to non-periodic data may result in significant boundary errors. To overcome this difficulty, we construct a smooth mth degree polynomial periodic continuation $C_m(\mathrm{R}eH)$ of R$eH(w)$ by requiring this continuation to be periodic on a wider domain. Then this periodically continued function is used to reconstruct ImH employing FFT and IFFT routines. ImH can also be used to reconstruct ReH; however, as can be seen from eq. (14), this would require the knowledge of R_∞. For this reason, it makes sense to reconstruct ImH from ReH unless it is known that $R_\infty = 0$. The idea of using periodic continuation was motivated by an example of the function $H(w) = \mathrm{e}^{-iaw}$, $a > 0$, that is not square integrable and only bounded, but satisfies the dispersion relations and has periodic real and imaginary parts [30]. Indeed, R$eH = \cos(aw)$, I$mH = -\sin(aw)$, $\mathrm{H}[\cos(aw)] = \sin(aw)$, and $H(w)\ \mathrm{H}[\sin(aw)] = -\cos(aw)$.

In the next section, we explain an idea of a periodic polynomial continuation and subsequent causality verification.

Periodic Polynomial Continuation and Causality Verification

In applications, the transfer function $H(w)$ is available on a finite bandwidth, $w_{min} \geq 0$, with a limited number N of discrete values. We start with the baseband case when $w_{min} \geq 0$. The approach can be generalized to the bandpass case when $w_{min} \geq 0$, as we show at the end of this section. Using spectrum symmetry, we can define $H(w)$ for $[-w_{max}, 0]$, since ReH and ImH are even and odd functions, respectively. For convenience, we rescale $H(w)$ to $H(x)$ defined on $x \in [-0.5, 0.5]$ by substitution $x = \frac{0.5}{w_{\max}}w$. Starting from R$eH$, we construct a new function $C_m(\mathrm{R}eH)$, a periodic polynomial continuation of ReH of degree m, that is the same as ReH on the interval $[-0.5, 0.5]$ and defined by an mth degree polynomial $P_m(x)$ on $[0.5, 0.5 + 2b]$ in such a way that this new function is periodic in the extended domain of length $1 + 2b$ and smooth up to order $m/2$ (m is even) at points ± 0.5. Given a function R$eH(x)$, available at a discrete set of points in a unit-length interval, its periodic mth degree polynomial continuation $C_m(\mathrm{R}eH)$ is defined by

$$C_m(\mathrm{R}eH)(x) = \begin{cases} \mathrm{R}eH(x), \quad x \in [0, 0.5] \\ \mathrm{R}eH(-x), \quad x \in [-0.5, 0] \\ P_m(x) = \sum_{l=0}^{m}\alpha_l(x - x_0)^l, \quad \frac{d^k}{dx^k}\mathrm{R}eH(0.5) = \frac{d^k}{dx^k}P_m(0.5), \\ \frac{d^k}{dx^k}\mathrm{R}eH(-0.5) = \frac{d^k}{dx^k}P_m(0.5 + 2b), \quad k = 0, \ldots, m/2, \end{cases} \tag{17}$$

where function $H(x)$ was reflected to $[-0.5, 0]$ as an even function and $1 + 2b$ is the period of the continuation. It may be more convenient to think about the continuation $C_m(\mathrm{R}eH)(x)$ defined on a symmetric interval $[-0.5, -b, 0.5 + b]$. The value of b that determines the length of the extended domain can be chosen depending on the behavior of $H(x)$ in the boundary regions around points ± 0.5. For periodic spectral continuations [34-39, 28] based on approximation of a function with a truncated Fourier series, the period of the continuation $1 + 2b$ is typically chosen as twice the length of the original interval (we have a unit interval in our case), so $2b = 1$ implies $b = 0.5$. This choice is not necessarily optimal since the error due to the selection of b depends on a function being approximated, but it is prominent in the literature (in particular, recommended in [36]), has error estimates [37], and a fast algorithm [39] developed. For smooth functions $H(x)$ that do not have wild oscillations in the boundary regions, the extended domain may be chosen even larger $b > 0.5$. In cases when $H(x)$ has high frequency oscillations or steep slopes in the boundary regions, b may be chosen smaller $0 < b < 0.5$ [34, 28]. In this work, we find that the same approach with the choice of b is applicable. In our examples, we use b ranging from $b = 0.00202$ to $b = 1$. The value of b may be tuned to get the better performance of the method. The default value $b = 0.5$ can be chosen first. To see if a smaller reconstruction error can be achieved with other values of b, b can be varied in small increments within the range $0 < b < 1$ following the aforementioned recommendations.

Since ReH is the even function, the polynomial P_m should be of an even degree m and the polynomial $\sum_{l=0}^{m}\alpha_l x^l$ should be an even function as well. Hence, all coefficients α_l with odd indices are zero. The remaining coefficients α_l with even indices are computed by requiring $P_m(x)$ and its derivatives up to the order $m/2$ to match function ReH and its corresponding derivatives at points ± 0.5. By symmetry, it is enough to consider only the point $x = 0.5$. For example, for $P_2(x) = a_2(x - x_0)^2 + a_0$, the unknown coefficients are a_2 and a_0 and they are computed by requiring P_2 and its first-order derivative P_2' to match ReH and $(\mathrm{R}eH)'$ at $x = 0.5$. For $P_4(x) = a_4(x - x_0)^4 + a_2(x - x_0)^2 + a_0$, the unknowns a_4, a_2, and a_0 are computed by requiring P_4, P_4', and P_4'' to match ReH, $(\mathrm{R}eH)'$, and $(\mathrm{R}eH)''$ at $x = 0.5$, respectively. A polynomial P_m has $m/2 + 1$ unknown coefficients that are found by requiring P_m and its derivatives up to order $m/2$ inclusively to have the same values as ReH and its corresponding derivatives at $x = 0.4$. To compute coefficients α_l of the polynomial $P_m(x)$, one needs to know function ReH and its derivatives. However, only discrete values of ReH are available. Derivatives of ReH can be approximated, for example, using one-sided finite differences [40], since only values of $H(x)$ to the left from point $x = 0.5$ are available.

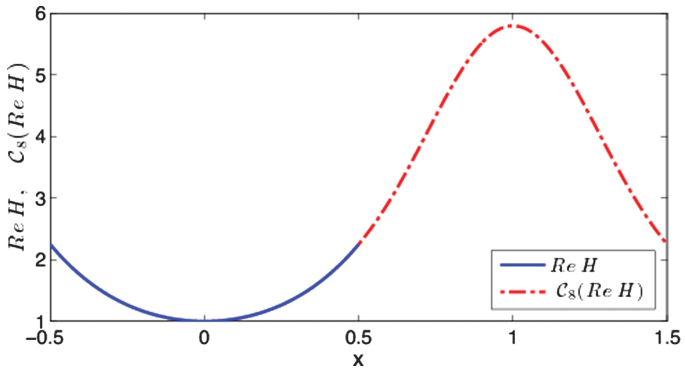

Fig. 1. Function $f(x) = 4x^4 + 4x^2 + 1$ and its periodic 8th degree polynomial continuation $C_8(f)(x)$ with $b = 0.2$ and $N = 501$.

Higher-order approximations of derivatives can be constructed using, for instance, Richardson extrapolation [40].

In Fig. 1, as an example, we show function $f(x) = 4x^4 + 4x^2 + 1$ and its periodic 8th degree polynomial continuation $C_8(f)(x)$ with $b = 0.2$. The period of the continuation is $1 + 2b = 1.4$. Moreover, the continuation $C_8(f)(x)$ and its derivatives up to 4th order are continuous at $x = \pm 0.5$.

Analysis section for more details]), and computing some norm $\|E_{C,m}\|$ (l_∞ or l_2 norm, for example) of the reconstruction error $E_{C,m}$, a decision then can be made whether the given transfer function $H(x)$, and, hence, $H(w)$, are causal or not depending on if $\|E_{C,m}\| < \varepsilon$ or not. In this work, we use l_∞ norm to analyze the error. The error estimates developed in the Error Analysis section are also given in terms of l_∞ norm.

This approach can be generalized to the bandpass regime with $w_{min} > 0$. In this case, $H(w)$ is available at a discrete set of points in $[w_{min}, w_{max}]$. Similar to the baseband case, we rescale $H(w)$ to $H(x)$ by substitution $x = \dfrac{0.5}{w_{\max}} w$. Then $H(x)$ is defined on $[a, 0.5]$, where $a = 0.5\dfrac{w_{\min}}{w_{\max}} > 0$. Since ReH is an even function, we have values of ReH on $[-0.5, -a]$ by spectrum symmetry. To define missing values of ReH in $[-a, a]$, we construct a polynomial $\tilde{P}_{m_0}$ of an even degree m_0 using a similar approach as for construction of P_m, in which we require $\tilde{P}_{m_0}$ to be an even function. Moreover, $\tilde{P}_{m_0}$ and its derivatives up to the order $m_0/2$ should match ReH and its corresponding derivatives at $x = \pm a$. The degree m_0 may be the same as m or different. In this work, we use $m_0 = m$. Then the periodic continuation $C_{m,m_0}(\mathrm{R}eH)$ is defined as follows.

$$
C_{m,m_0}(\mathrm{R}eH)(x) = \begin{cases} \mathrm{R}eH(x), \quad x \in [a, 0.5] \\ \mathrm{R}eH(-x), \quad x \in [-0.5, -a], \\ P_m(x) = \sum\limits_{l=0}^{m} \alpha_l (x - x_0)^l, \quad x \in [0.5, 0.5 + 2b], \quad x_0 = 0.5 + b, \\ \tilde{P}_{m_0}(x) = \sum\limits_{k=0}^{0} \beta_k x^k, \quad x \in [-a, a], \\ \dfrac{d^k}{dx^k}\mathrm{R}eH(0.5) = \dfrac{d^k}{dx^k} P_m(0.5), \quad k = 0, \ldots, m/2, \\ \dfrac{d^k}{dx^k}\mathrm{R}eH(-0.5) = \dfrac{d^k}{dx^k} P_m(0.5 + 2b), \quad k = 0, \ldots, m/2, \\ \dfrac{d^l}{dx^l}\mathrm{R}eH(\pm a) = \dfrac{d^l}{dx^l} \tilde{P}_{m_0}(\pm a), \quad l = 0, \ldots, m_0/2. \end{cases} \tag{20}
$$

When the continuation $C_m(\mathrm{R}eH)$ is constructed, its Hilbert transform $\mathrm{H}[C_m(\mathrm{R}eH)]$ can be computed on $[-0.5, 0.5 + 2b]$ by FFT/IFFT routines to approximate ImH using eq. (15). This would require finding the discrete Fourier transform of $C_m(\mathrm{R}eH)$, multiplying the obtained Fourier coefficients by $isgn(k)$, where k is the wave number [see eq. (16)], consequently computing the inverse Fourier transform, and multiplying it by -1. The result $-\mathrm{H}[C_m(\mathrm{R}eH)]$ is then compared with ImH on the original interval $[-0.5, 0.5]$.

Denote by $E_{C,m}$ the error in reconstructing ImH from ReH using an mth degree polynomial continuation $C_m(\mathrm{R}eH)$:

$$
\begin{aligned} E_{C.m}(x) &= \mathrm{I}mH - (-\mathrm{H}[C_m(\mathrm{R}eH)(x)]) \\ &= \mathrm{I}mH + \mathrm{H}[C_m(\mathrm{R}eH)(x)], \end{aligned} \tag{18}
$$

where $x \in [-0.5, 0.5]$. For completeness, we also introduce the error E of reconstructing ImH from ReH without any continuation used:

$$
E(x) = \mathrm{I}mH + H[\mathrm{R}eH(x)], \quad x \in [-0.5, 0.5]. \tag{19}
$$

Given a tolerance $\varepsilon > 0$ (based on the accuracy of the data and the continuation overall, and its smoothness [see the Error

Again, by periodicity, we can think that the continuation $C_{m,m_0}(\mathrm{R}eH)(x)$ is defined on a symmetric interval $[-0.5-b, 0.5 + b]$. Having the continuation $C_{m,m_0}(\mathrm{R}eH)(x)$ constructed, one can verify causality of H using a similar approach as for the baseband case: employing the continuation $C_{m,m_0}(\mathrm{R}eH)(x)$ instead of ReH to reconstruct ImH via eq. (15) and comparing the result with ImH on the original interval $[-0.5, 0.5]$. In other words, one needs to compute the discrete Fourier transform $\mathrm{F}[C_{m.m_0}(\mathrm{R}eH)(x)]$ using FFT, and multiply the obtained Fourier coefficients by $isgn(k)$. Computing the inverse discrete Fourier transform of the result using IFFT and multiplying it by -1 will give the negative Hilbert transform of the continuation, $-\mathrm{H}[C_{m.m_0}(\mathrm{R}eH)]$, which should be compared with ImH (I), $x \in [-0.5,0.5]$. We use the same definition (18) of the reconstruction error $E_{C,m}$ as for the baseband case. If this error is greater than the causality threshold ε, the transfer function $H(x)$ is noncausal. Otherwise, we say that causality is satisfied within the error less or equal than ε. The bandpass case is considered in the transmission line example later in this paper, where the transfer function $H(w)$ is only available for $w > 0$.

Next, we present an analysis of the error in approximation of ImH by $-\mathrm{H}[C_m(\mathrm{R}eH)]$ or $-\mathrm{H}[C_{m.m_0}(\mathrm{R}eH)]$ when only a

discrete set of values of H is available in the presence of a noise or approximation errors in the data.

Error Analysis

Assume that the data for $H(w) = ReH(w) + iImH(w)$ are available on $[w_{min}, w_{max}]$, $w_{min} \geq 0$, at a discrete set of frequencies $w_j, j = 1,\ldots,N$. Consider first the case when $w_{min} = 0$. After rescaling from w to x and using spectrum symmetry, we obtain the function $H(x)$, whose domain is $\Omega = [-0.5, 0.5]$ and values are available at $x_j \in \Omega, j = 1,\ldots, 2N-1$. Denote by $\Omega^c = [-0.5, -b, 0.5 + b]$ the domain of a single period of a polynomial continuation $C_m(ReH)(x)$ constructed by using a polynomial $P_m(x)$ defined in eq. (17). The continuation is defined on a wider domain Ω^c that contains Ω and available at points $\tilde{x}_j \in \Omega^c, j = 1,\ldots,2M+1, M > N$. Moreover, $\tilde{x}_j = x_j$ if $\tilde{x}_j \in \Omega$. When $w_{min} > 0$, we denote by $\Omega = [-0.5, -a] \cap [a, 0.5]$. In this case, $ReH(x)$ also needs to be approximated around zero by another polynomial $\tilde{P}_{m_0}$ defined in eq. (20) for $x \in [-a, a]$, $a = 0.5\dfrac{w_{min}}{w_{max}}$, since the part of the spectrum around zero is missing.

Our goal is to bound the error in the approximation of $ImH(x)$ by $-H[C_m(ReH)(x)]$ or $-H[C_{m,m_0}(ReH)(x)]$ for a causal function $H(x)$ in the domain Ω. Because of the spectrum symmetry, the error is the same on the interval $x \in [0, 0.5]$ and, hence, on $w \in [0, w_{max}]$. In the bandpass case when $w_{min} \geq 0$, the domain of interest is $x \in [a, 0.5]$ or $w \in [w_{min}, w_{max}]$, respectively.

There are several sources of the error. The first error E_p is due to approximation of derivatives of $ReH(x)$ needed for construction of polynomials $P_m(x)$ and $\tilde{P}_{m_0}(x)$. Consider the mth degree polynomial $P_m(x)$ first. Since we use the same samples of H at $x_j \in \Omega$, the error E_p is zero on Ω and nonzero on $\Omega^c \setminus \Omega$. If the derivatives of ReH are approximated using finite difference formulas of order $O(h^r)$, $r = 1, 2,\ldots$ with $h = \dfrac{0.5}{N-1}$, then the polynomial continuation is accurate within the error $O(h^r)$ and has order $m/2$ of smoothness at boundary points $x = \pm 0.5$. Similarly, constructing a polynomial $\tilde{P}_{m_0}(x)$ for $x \in [-a, a]$ using the same order finite difference approximations results in the error of the same order $O(h^r)$. Then $E_p = O(h^r)$. If $m = m_0$, then both polynomials $P_m(x)$ and $\tilde{P}_m(x)$ have the same smoothness order $m/2$ at $x = \pm 0.5$ and $x = \pm a$, respectively.

The second error E_F comes from approximating the function $C_m ReH(x)$ or $C_{m,m_0}(ReH)(x)$ by a $2M$-mode Fourier series, which is computed by employing an FFT routine. This error depends primarily on the smoothness of the function on the entire domain Ω^c where the Fourier series is constructed. For a function g with period $1 + 2b$ and k continuous derivatives, the error in approximation of g by the first $2M$-mode Fourier series, denoted by $\hat{g}_M$, follows from Jackson theorems [41]:

$$\|E_F\|_{L^\infty(\Omega^c)} = \|g - \hat{g}_M\|_{L^\infty(\Omega^c)} \leq \frac{\pi}{2}\left(\frac{1+2b}{2\pi}\right)^k \left(\frac{1}{M}\right)^k \left\|g^{(k)}\right\|_{L^\infty(\Omega^c)}. \quad (21)$$

This error bound shows that as b increases, the error may also increase. On the other hand, as b approaches a value of 1, the Gibbs phenomenon does not allow the error $\|g - \hat{g}_M\|_{L^\infty(\Omega^c)}$ to decay rapidly if function g is nonperiodic. An optimal value of b depends on the specific function g being approximated [36, 37]. The value $b = 0.5$ can be chosen for convenience, since this value is often used in the literature, especially in the case of singular value decomposition (SVD)-based Fourier continuations [39, 28, 42].

Denote by $g = C_m(ReH)(x)$ and $\hat{g} = \hat{C}_m(ReH)(x)$ its $2M$-mode Fourier approximation. Let ReH have k_1 continuous derivates on Ω. Then the continuation $C_m(ReH)(x)$ has $k = \min(k_1, m/2)$ continuous derivatives since the polynomial P_m of order m has up to $m/2$ continuous derivatives at $x = \pm 0.5$. Therefore, smoothness of g on Ω^c depends on smoothness of ReH and the order m of the polynomial P_m. If $g = C_{m,m_0}(ReH)(x)$ is used instead, then with the choice $m_0 = m$, this continuation has the same order of smoothness, otherwise $k = \min(k_1, m/2, m_0/2)$.

The frequency responses may be known with some error E_d. This is the third source of the error. This error may be due to experimental measurement inaccuracies or approximation and discretization in case of finite element numerical simulations. This implies that both ReH and ImH are known with the error E_d on Ω. Since the polynomial continuations are constructed with the error E_p due to finite difference approximation of derivatives of ReH and this error is on $\Omega^c \setminus \Omega$, we can write the following error bound:

$$\left\|(g + E_p + E_d) - \hat{g}_N\right\|_{L^\infty(\Omega^c)} = \left\|(g - \hat{g}_N) + E_p + E_d\right\|_{L^\infty(\Omega^c)} \leq \|(g - \hat{g}_N)\|_{L^\infty(\Omega^c)} + \left\|E_p\right\|_{L^\infty(\Omega^c)} + \|E_d\|_{L^\infty(\Omega)}, \quad (22)$$

where $g = C_m(ReH)(x)$ or $g = C_{m,m_0}(ReH)(x)$.

Further, to check causality, we compute $-H[C_m(ReH)(x)]$ or $-H[C_{m,m_0}(ReH)(x)]$ to approximate $ImH(x)$ on Ω. The Hilbert transform is calculated spectrally using the convolution form (15) and the fact that $F\left[\dfrac{1}{\pi x}\right] = i\,sgn(k)$, as follows. The discrete Fourier transform of $C_m(ReH)(x)$ or $C_{m,m_0}(ReH)(x)$ is computed using FFT and then Fourier coefficients of $C_m(ReH)(x)$ or $C_{m,m_0}(ReH)(x)$ are multiplied by $isgn(k)$ with the subsequent application of IFFT to the result to compute its inverse discrete Fourier transform and multiplication by -1 to get $-H[C_m(ReH)(x)]$ or $-H[C_{m,m_0}(ReH)(x)]$, respectively. For this reason, the error in computing the Hilbert transform of $C_m(ReH)(x)$ or $C_{m,m_0}(ReH)(x)$ is dominated by approximation of these functions with their corresponding truncated Fourier series, for which the error bound is given in (22), where the noise E_d in data and discretization error E_p are taken into account.

Therefore, we can write the following error bound for approximation of ImH by $-H[C_m(ReH)(x)]$ on Ω:

$$\left\|(ImH(x) + E_d) - \left\{-H[C_m(ReH)(x) + E_p + E_d]\right\}\right\|_{L^\infty(\Omega)} \leq \|C_m(ReH)(x) - C_m(\widehat{ReH})(x)\|_{L^\infty(\Omega^c)} + \left\|E_p\right\|_{L^\infty(\Omega^c)} + \|E_d\|_{L^\infty(\Omega)}$$

$$\leq \frac{\pi}{2}\left(\frac{1+2b}{2\pi}\right)^k\left(\frac{1}{M}\right)^k\left\|(C_m(\mathrm{R}eH))^k\right\|_{L^\infty(\Omega^c)} + \left\|E_p\right\|_{L^\infty(\Omega^c)} + \|E_d\|_{L^\infty(\Omega)}$$

Similar error estimates can be written if $C_{m,m_0}(\mathrm{R}eH)$ is used instead. Therefore, we can formulate the following result.

Theorem. Consider a rescaled transfer function $H(x) = \mathrm{R}eH(x) + i\mathrm{I}mH(x)$ whose discrete values are available at equally spaced points $x_j \in \Omega$, $\Omega = [-0.5,0.5]$, $j = 1,\ldots, 2N-1$, that are accurate within the error E_d. Assume that $H(x)$ has k_1 continuous derivatives on Ω. Construct a periodic mth degree polynomial continuation C_m (ReH) of ReH on $\Omega^c = [-0.5, -b, 0.5 + b]$, $b > 0$, defined in (17). Assume that derivatives of ReH up to order $m/2$ needed for polynomial construction are approximated by finite difference formulas accurate to $O(h^r)$, where $h = \dfrac{0.5}{N-1}$, r = 1, 2,.... Then the error in approximation of I$mH(x)$ by $-\mathrm{H}[C_m(\mathrm{R}eH)](x)$ on Ω computed in the presence of errors E_d and E_p has the upper bound

$$\frac{\pi}{2}\left(\frac{1+2b}{2\pi}\right)^k\left(\frac{1}{M}\right)^k\left\|(C_m(\mathrm{R}eH))^{(k)}\right\|_{L^\infty(\Omega^c)} + \tilde{C}h^r + \|E_d\|_{L^\infty(\Omega^c)}, \quad (23)$$

where $k = \min(k_1, m/2)$, $M = \dfrac{1+2b}{2h} > N$, $\left\|E_p\right\|_{L^\infty(\Omega^c)} \leq \tilde{C}h^r$, and $\tilde{C}$ is some constant that depends on a certain derivative of ReH.

If function $H(x)$ has missing values in $x \in [-a, a]$, $0 < a < 0.5$ and another polynomial $\tilde{P}_{m_0}(x)$ of degree m_0 computed using derivatives of ReH accurate within $O(h^r)$ is used to approximate $H(x)$ on $[-a, a]$, the error estimates are similar, perhaps with a different constant $\tilde{C}$:

$$\frac{\pi}{2}\left(\frac{1+2b}{2\pi}\right)^k\left(\frac{1}{M}\right)^k\left\|(C_{m,m_0}(\mathrm{R}eH))^{(k)}\right\|_{L^\infty(\Omega^c)} + \tilde{C}h^r + \|E_d\|_{L^\infty(\Omega^c)}, \quad (24)$$

where $k = \min(k_1, m/2, m_0/2)$.

This result implies that the error in reconstruction of ImH depends on the smoothness of the periodic polynomial continuation C_m(ReH), on the number $2N-1$ of samples on Ω, the choice of the continuation parameter b, and, consequently, the number $2M$ of samples on Ω^c. This is given by the first term in (23). The error also depends on the accuracy of the polynomial continuation [second term of order $O(h^r)$] and accuracy of the given data (the last term with $\|E_d\|_{L^\infty(\Omega^c)}$). Since the smoothness of the polynomial continuation depends on the degree of the polynomials P_m and $\hat{P}_{m_0}$, the higher degrees m and m_0 are, the smoother the continuation will be, and, as a consequence, the smaller error should be in the reconstruction of ImH at the boundary due to mismatch of values of H and its derivatives at $x = \pm 0.5$ for nonperiodic functions H.

The largest error among E_F, E_d, and E_p can be used to define the threshold

$$\varepsilon = \max\left\{\|E_F\|_{L^\infty(\Omega^c)}, \|E_d\|_{L^\infty(\Omega)}, \left\|E_p\right\|_{L^\infty(\Omega^c)}\right\}$$

for the reconstruction error $E_{C,m}$, defined in (18), above which the frequency responses will be considered noncausal. If the error is smaller than ε, the data are considered causal within the error ε. This choice of the threshold may be too high, and the smoothness order k_1 of the data may not be known in practice. k_1 can be estimated from the growth rate of the reconstruction error $E_{C,m}$ when N, $N/2$, $N/4$, and so on samples are used with the same b. For practical purposes, the threshold ε can be chosen to coincide with the accuracy of the data (accuracy of measurements or numerical simulations).

In the Numerical Examples section, we test the polynomial continuation method for causality verification on several analytic and simulated causal and noncausal examples to show that the approach with the periodic continuation is able to decrease significantly the error at the boundary of the frequency interval that is due to the lack of out-of-band frequency responses. Causal transfer functions are used for validation of the method and they present a so-called ideal causality test. We also impose localized smooth causality violations modeled by a Gaussian function and show that the approach is capable of detecting them even when the amplitude of such violations is small.

Numerical Examples

In this section, we apply the proposed technique to several functions, causal and noncausal, to verify effectiveness of the proposed method.

A. Four-Pole Example

To test the performance of the proposed technique, we consider a transfer function with four poles defined by

$$H(w) = \frac{r_1}{iw+p_1} + \frac{\bar{r}_1}{iw+\bar{p}_1} + \frac{r_2}{iw+p_2} + \frac{\bar{r}_2}{iw+\bar{p}_2},$$

with $r_1 = 1 + 3i$, $p_1 = 1 + 2i$, $r_2 = \dfrac{2}{3} + \dfrac{1}{2}i$, $p_2 = \dfrac{1}{2} + 5i$. Since the poles of $H(w)$ are located in the upper half w-plane at $\pm 2 + i$ and $\pm 5 + \dfrac{1}{2}i$, this function is causal as a sum of four causal transforms. H is sampled on $[0, w_{max}]$, with w_{max} = 10 GHz. Using the spectrum symmetry, ReH is reflected to $[-w_{max}, 0]$ as an even function, and the interval $[-w_{max}, w_{max}]$ is rescaled to $[-0.5, 0.5]$. ReH is shown in Fig. 2a. Superimposed is its periodic 8th degree polynomial continuation C_8 (ReH)(x) with $b = 1$. In Fig. 2b, we plot ImH and its reconstruction $-\mathrm{H}[C_8(\mathrm{R}eH)(x)]$ using the continuation. For comparison, we also show the result of applying the Hilbert transform to ReH directly without any continuation, which is computed using the Matlab built-in function *hilbert*. It is clear that agreement between ImH and $-\mathrm{H}[C_8(\mathrm{R}eH)(x)]$ is much better than between ImH and $-\mathrm{H}[\mathrm{R}eH(x)]$, especially in the boundary region.

Next, we analyze the dependence of the quality of reconstruction on the smoothness of the continuation given by the polynomial degree m. In Fig. 3, we plot the reconstruction error $E_{C,m}$, defined in (18), for polynomial periodic continuations of degrees m = 2, 4, 6, and 8. For comparison, we also include the error E, defined in (19), when no continuation is used. The results indicate that using a periodic continuation, we are able to significantly reduce the error everywhere on the given interval but especially in the boundary region. The error

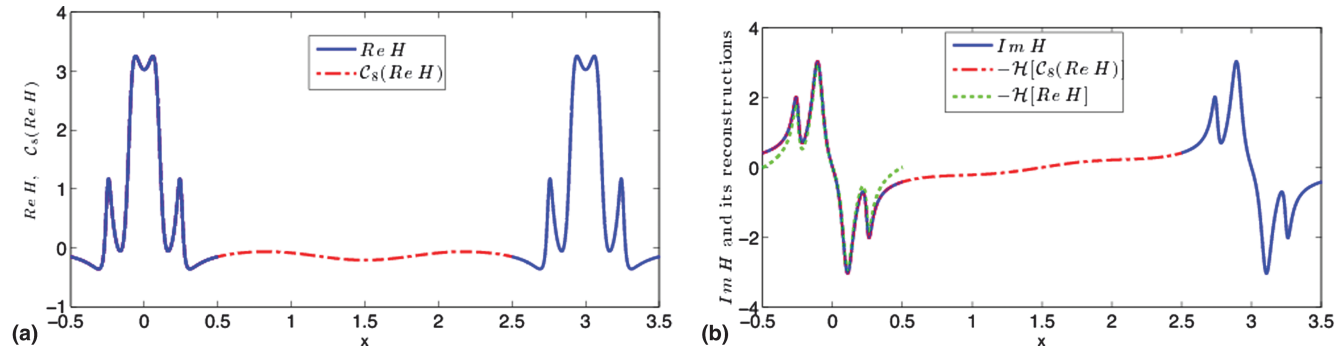

Fig. 2. (a) R$eH(x)$ and its periodic 8th degree polynomial continuation C_8 (ReH) (x) in the four-pole example with N = 1001, b = 1 shown on [−0.5, 3.5]. (b) ImH and its reconstructions $-\mathrm{H}[C_8(\mathrm{R}eH)(x)]$ and $-\mathrm{H}[\mathrm{R}eH(x)]$ with and without periodic continuation, respectively.

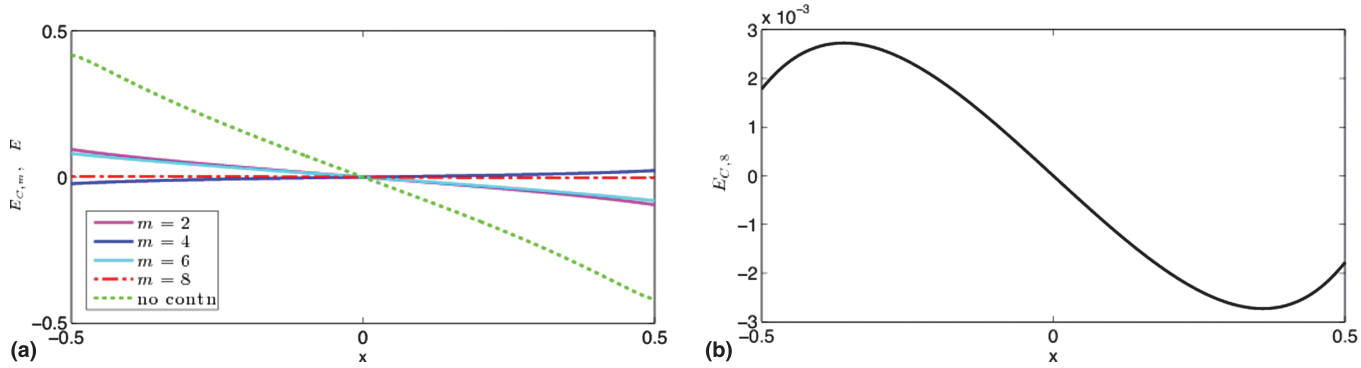

Fig. 3. (a) Errors $E_{C,m}$ in reconstruction of ImH in the four-pole example using continuation C_m (ReH)(x)) with polynomials of degree m = 2, 4, 6, 8, and b = 1, and E from the direct computation of Hilbert transform (without continuation) using Matlab function *hilbert*. (b) Zoom-in of the error $E_{C,8}$ (x).

is shown to decrease as the polynomial degree m increases, though not monotonically in this example. Specifically, the error $E_{C,2}$ with the 2nd degree polynomial continuation is about 4 times smaller than the error E without periodic continuation, while using 8th degree polynomial continuation reduces the error E by 100 times. This is in agreement with the error bound (21) that decreases as k increases. In Fig. 3b, we show the reconstruction error $E_{C,8}$ that does not exceed $3 \cdot 10^{-3}$ on the entire interval. We say that the given transfer function H (x), and, hence, H (w), are causal with the error at most $3 \cdot 10^{-3}$. Even though this error is not very small, such accuracy may be enough for some experimental results where it is not possible to get extremely high accuracy in measurements. Since the accuracy is higher for higher m, in what follows, we fix m = 8 and use it to construct polynomial continuations in other examples. Higher values of m can be used to get more accuracy. At the same time, we find that the reconstruction error $E_{C,m}$ does not significantly depend on the resolution of data [i.e., the number of samples N, once enough points are used to represent $H(x)$]. The order of accuracy of derivative approximation also has a weak effect on the quality of reconstruction. Therefore, in this example, the error is dominated by the error E_F in approximation of a function by a truncated Fourier series, which decreases as the smoothness of the function increases. See the Error Analysis section for more information.

B. Transmission Line Example

We consider a uniform transmission line segment of length L = 5 cm having the following per-unit-length parameters: L = 5.2 nH/cm, C = 1.1 pF/cm, R = 1.3 Ω/cm, and G = 0. This example was used in [25] to test a causality tool based on generalized dispersion relations with subtractions. The frequency is sampled on the interval (0, 9.0] GHz. The scattering matrix is computed using Matlab function rlgc2s. The element $H(w) = S_{11}(w)$ is selected for analysis. The model used in the function rlgc2s does not allow one to obtain the value of the transfer function at w = 0 (DC), but it is possible to sample it from any small nonzero frequency $w_{min} > 0$, so we have the bandpass case. Since the magnitude of S_{11} has to be bounded by 1, the value at w = 0 should be finite. The situation when a part of the low frequency response is missing can occur either in experimental measurements or simulations.

As was explained in the Periodic Polynomial Continuation and Causality Verification section, we use spectrum symmetry of $H(w)$ to get values of $H(w)$ for negative frequencies $[-w_{max}, -w_{min}]$. With the substitution $x = \dfrac{0.5}{w_{\max}} w$, we rescale $H(w)$ to $H(x)$ defined on $[-0.5, -a] \cap [a, 0.5]$. As with the baseband case, we use ReH to reconstruct ImH, since it does not require the value of H at infinity. The missing part in $[-a, a]$ is approximated by an even degree polynomial $\tilde{P}_{m_0}$ defined

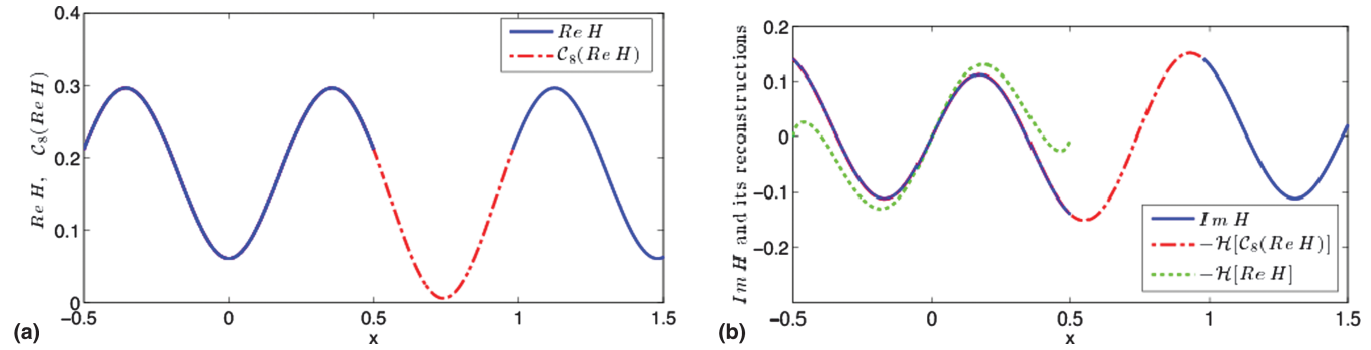

Fig. 4. (a) R$eH(x)$ and its 8th degree periodic polynomial continuation C_8 (ReH) in the transmission line example with $N = 1000$, $b = 0.24$ shown on $[-0.5, 1.5]$. (b) I$mH(x)$ and its reconstructions $-H[C_8(\mathrm{R}eH)(x)]$ with continuation and $-H[\mathrm{R}eH(x)]$ without continuation.

in (20) with $m_0 = m = 8$. Fig. 4a shows R$eH(x)$ together with $C_{8,8}$(ReH), whereas I$mH(x)$ and its reconstruction $-H[C_{8,8}(\mathrm{R}eH)]$, using continuation superimposed with reconstruction $-H[\mathrm{R}eH]$ without continuation, are presented in Fig. 4b.

Clearly, using continuation helps reduce the reconstruction error on the entire frequency interval. The corresponding errors $E_{C,8}$ and E are presented in Fig. 5. The results indicate that 8th degree polynomial continuation allows one to reduce the overall reconstruction error by about 200 times. The transfer function in this case is causal, with the error at most 7×10^{-4}.

It should be noted that even though the reconstruction error in the boundary regions close to w_{max} depends primarily on the smoothness of the continuation (i.e., the degree m of the polynomial P_m used to construct the continuation), and much less on data resolution, the accuracy of reconstruction in the region near $x = 0$ strongly depends on the resolution and proximity of w_{min} to zero. As the number N of samples increases, w_{min} decreases (in our test $w_{min} = w_{max}/N$), and the error in reconstruction near $x = 0$ also decreases as a function of $1/N$. We experimented with N ranging from 70 to 2,000 and found that for small N, the error around $x = 0$ decreases as a function of $1/N^3$, while for large values, it behaves as $1/N$. Hence, in this example, the discretization error $E_p = O(h^r)$ that defines the accuracy of construction of the polynomial $\tilde{P}_{m_0}$ for $x \in [-a, a]$ plays a more important role for x around 0 than the smoothness of the continuation.

Next, we test the sensitivity of the method to detect causality violations by artificially imposing a localized causality violation modeled by a Gaussian function [23, 25]

$$a\exp\left(-\frac{(x-x_0)^2}{2\sigma^2}\right), \quad 6\sigma = 10^{-2}, \tag{25}$$

where a and x_0 are an amplitude and location of a perturbation. Here $\sigma = 10^{-2}/6$ is the standard deviation of the Gaussian, so that the "support" of such perturbation is 10^{-2}, a very small number. Outside this support, the perturbation is very close to zero. We add this perturbation to R$eH(x)$ and keep I$mH(x)$ unchanged. A symmetric perturbation is imposed at $-x_0$. We note that the Gaussian function is infinitely smooth and is typically difficult to detect smooth causality violations [25]. We vary the amplitude a of the perturbation to find how small causality violations can be detected, for example, using 8th degree polynomial continuations C_8R$eH(x)$. The results with $x_0 = 0.1$, $a = 10^{-2}$, 10^{-3}, and 10^{-4} are shown in Fig. 6.

We can clearly see that the approach with a polynomial periodic continuation gives superior results over the approach without a continuation. For larger amplitude $a = 10^{-2}$, both methods, with and without continuation, allow one to detect the causality violation location by developing spikes there. The method with the continuation maintains much smaller error away from the region where the violation is imposed, while

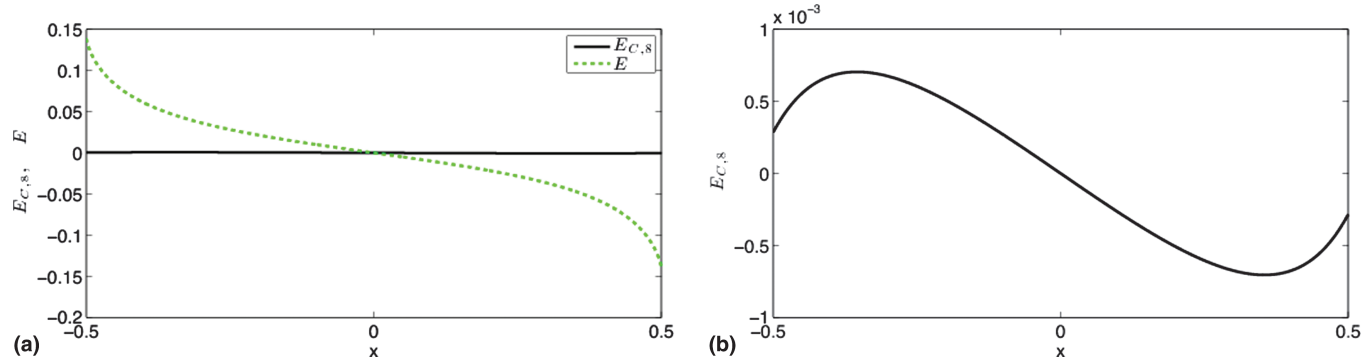

Fig. 5. (a) Reconstruction errors $E_{C,8}$ and E in the transmission line example with and without continuation. (b) Zoom-in of the error $E_{C,8}$.

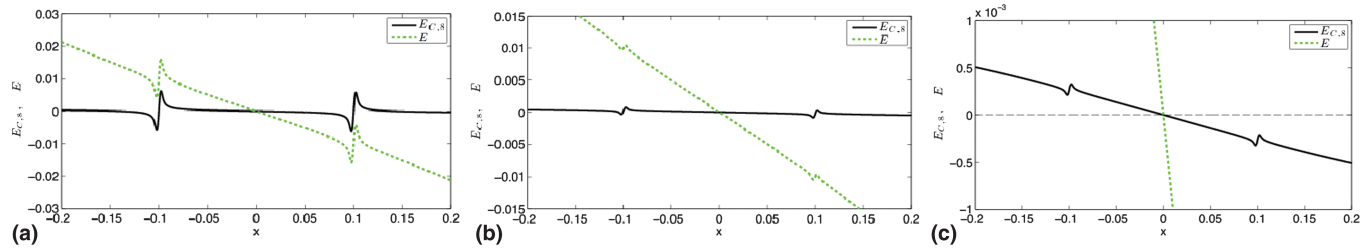

Fig. 6. Errors $E_{C,8}$ and E in the transmission line example with the imposed Gaussian causality violation (25) of amplitudes (a) $a = 10^{-2}$, (b) $a = 10^{-3}$ and (c) $a = 10^{-4}$.

without continuation, the magnitude of the error is even higher away from the location of causality violation, which makes it essentially impossible to differentiate between true causality violation and just error variation that is due to the truncation of the domain in this case. When $a = 10^{-3}$, the difference between results obtained using the two approaches is even more pronounced. The method with the continuation successfully detects the violation. Even though the error with the method without continuation also produces spikes at the location of the violation, the magnitude of the error is much bigger than the size of the spike, so this method fails to detect the causality violation. With even smaller amplitude, $a = 10^{-4}$, the approach with a polynomial continuation is still able to detect causality violation locations by developing spikes in the reconstruction error at the appropriate values of x, but these spikes are of about the same magnitude as the surrounding error, so they may not be understood as indicators of causality violations. The approach without continuation is not essentially able to detect the causality violation of this small size at all.

The sensitivity of the method to detect small causality violations depends on the fact if the method is capable of producing appropriate size disturbances in the error at the locations of causality violations (spikes in our case, since we use localized Gaussian perturbations of a causal function) with the error on the rest of the domain of smaller size. To analyze this, we do the following. With the causality violations located at ± 0.1, we fix control points, for example, $x = -0.5$ (boundary), $x = -0.4$, $x = -0.3$, and $x = -0.2$, vary the degree of the polynomial from $m = 2$ to $m = 8$, and compute the reconstruction error $E_{C,m}$ at the control points. The logarithmic plot of these errors is given in Fig. 7. The values at $m = 0$ correspond to reconstruction

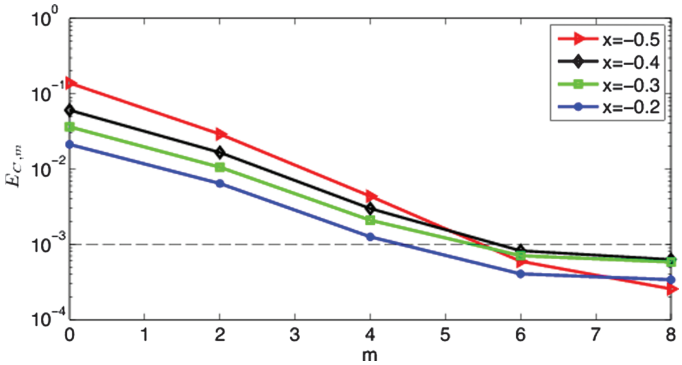

Fig. 7. Errors $E_{C,m}$ in the transmission line example with $m = 2$, 4, 6, and 8 at control points $x = -0.5$, -0.4, -0.3, and -0.2.

errors obtained without using continuation. The plot shows that as the degree m of the polynomial (i.e., smoothness of the polynomial continuations) increases, the reconstruction error decreases at all control points, especially at the boundary. In particular, for $m \geq 6$, the error at all control points is below 10^{-3} (shown by the dashed line), which implies that the method with the polynomial continuation of degree at least 6 can detect causality violations of the amplitude 10^{-3} or higher. The plot also suggests that with higher values of m, the method should become sensitive to even smaller causality violations.

In papers [23-25], the generalized dispersion relations with subtractions were used to check causality of raw frequency responses. The authors provide explicit error estimates to account for finite frequency resolution (discretization error in computing Hilbert transform integral) and finite bandwidth (truncation error due to using only a finite frequency interval instead of the entire frequency axis), and to make the causality violations unbiased from numerical discretization and domain truncation errors. The authors show that with more subtractions, one can make the truncation error arbitrarily small, but the discretization error that is fixed by the resolution of given frequency responses does not go away. They report that if causality violations are too small and smooth, using more subtractions may not affect the overall error, since it is then dominated by the discretization error. In addition, even placing more subtraction points in the boundary regions close to $\pm w_{max}$ may not affect the truncation error, and it may not be small, since the out-of-band samples are missing. In the current work, we are able to significantly decrease boundary artifacts by constructing smooth, periodic polynomial continuations. Moreover, the higher degree m of the continuation polynomial is, the smaller overall reconstruction can be obtained, especially in the boundary region. The method also allows one to detect smooth causality violations (Gaussian is an infinitely smooth function). Even though using 8th degree periodic polynomial continuation allows one to reach reconstruction error only on the order of 10^{-5} and the approach is capable of detecting causality violation of the amplitude up to 10^{-4}, numerical experiments, as well as work [28], show that with higher values of degree m and smoother continuations, the reconstruction error $E_{C,m}$ can be decreased to increase the sensitivity of the method to small causality violations. The discretization error and a noise in data also affect the performance of the method, since they contribute to the upped bound (24) of the reconstruction error below which the method is not able to differentiate between causality violations and the discretization error (see the Error Analysis section for more details).

C. Finite Element Model of a Dynamic Random Access Memory Package

This example uses a scattering matrix S of a dynamic random access memory (DRAM) package with 110 input and output ports, which was generated by a Finite Element Method (courtesy of Micron Technology Inc). The values of the scattering matrix are available at $N = 100$ equally spaced frequency points ranging from $w_{min} = 0$ to $w_{max} = 5$ GHz. We apply the technique to the S parameter $H(w) = S(100, 1)$ that relates the output signal from port 100 to the input signal at port 1 as a function of frequency w. The procedure can be extended to other elements of S by applying the method to every element of the scattering matrix. After rescaling frequencies to $[-0.5, 0.5]$, we obtain function $H(x)$.

ReH (x) is plotted in Fig. 8a superimposed with C_8(Re$H(x)$), where we used $b = 0.0202$. Fig. 8b contains Im$H(x)$ and the result of application of the Hilbert transform to C_8(Re$H(x)$). For comparison, we also plot H[Re$H(x)$] without any continuation. The reconstruction errors $E_{C,8}$ and E are shown in Fig. 9a. The results indicate that periodic continuation allows one to maintain a small uniform error on the order of 10^{-5} away from the boundary that is about 10 times smaller than the error obtained without using continuation. However, the error in the boundary region in this example is bigger, with $b > 0$ compared with $b = 0$. This can be explained by the fact that both Re$H(x)$ and Im$H(x)$ have steep slopes at the boundary that are most likely signs of a discontinuity typical for transfer functions of real-life high-speed interconnects. A limited smoothness of a continuation (for an 8th degree polynomial, the continuation is smooth only up to a 4th order derivative at end points) is not enough to resolve the discontinuity and remove boundary effects. Smoother periodic continuations are needed to handle the error at the boundary in this example. In Fig. 9b, we analyze the reconstruction error $E_{C,8}$ as the length b of the extended domain varies. As b increases from $b = 0$ to $b = 8h$ with $h = 0.0051$, we observe that the error away from the boundary decreases and reaches its minimum (optimal value) around $b = 4h$ and then starts to increase. The error at the boundary increases monotonically with b.

In this example, our method shows that the frequency responses are causal within 10^{-5} error away from the boundary (about 20%), whereas the error in the boundary region is on the order of 10^{-3}. Even though the error is not very small, this accuracy may be acceptable in practical situations when experimental data are used and it is not possible to achieve very high accuracy in measurements.

The relatively large reconstruction error at the boundary comes from low smoothness order of the transfer function and the polynomial continuation, as well as from low resolution.

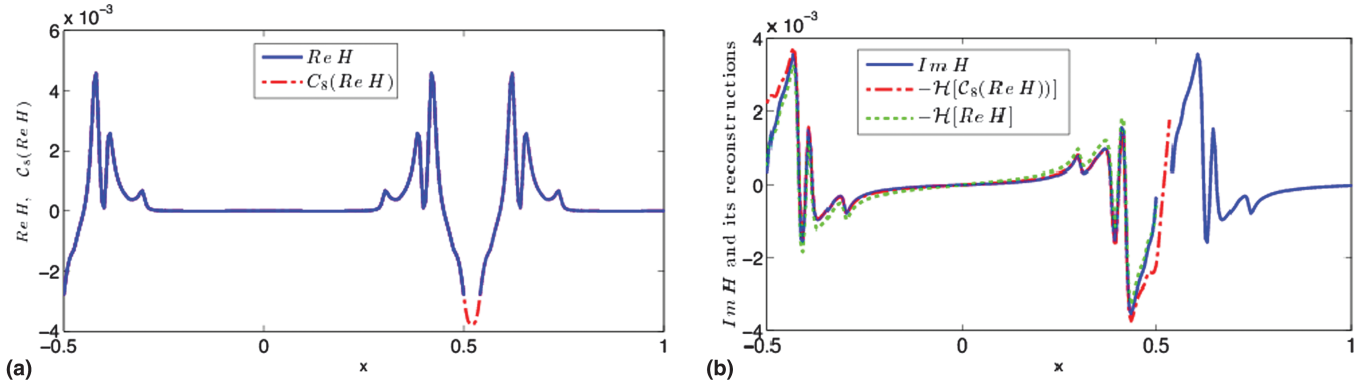

Fig. 8. (a) Re$H(x)$ and its periodic 8th degree polynomial continuation C_8 (ReH)(x) in the example of a finite element model of a DRAM package with $N = 11$, $b = 0.0202$ shown on $[-0.5, 1]$. (b) Im$H(x)$ superimposed with H$[C_8(\mathrm{Re}H)(x)]$ and H[ReH].

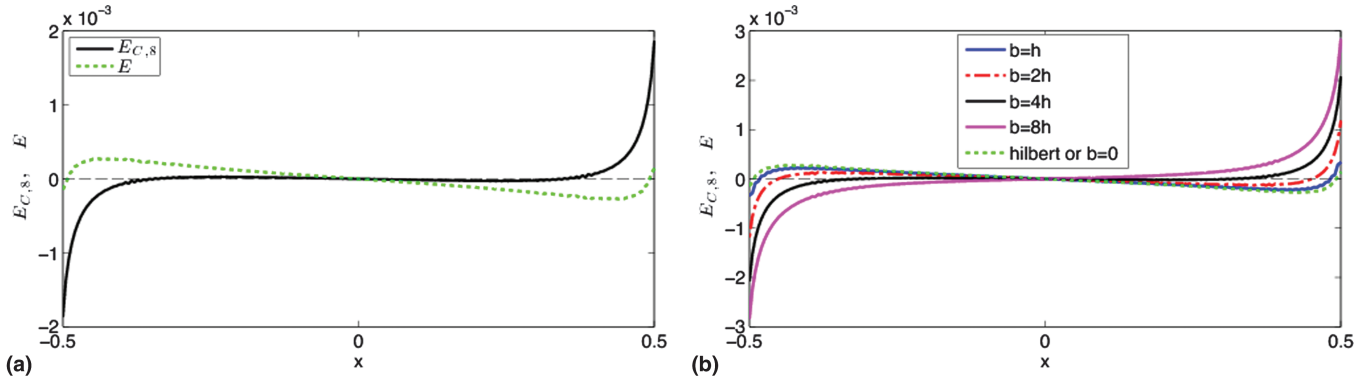

Fig. 9. (a) Error $E_{C,8}$ of approximation of ImH (x) by $-$H$[C_8(\mathrm{Re}H)]$ with a periodic 8th degree polynomial continuation, $N = 100$, $b = 0202$ compared with the error E with H[ReH] without periodic continuation in the example of a finite element model of a DRAM package. (b) Errors $E_{C,8}$ and E for various length of the extended domain: $b = 0$ (no continuation), $b = h$, $2h$, $4h$, and $8h$, where $h = 0.0051$.

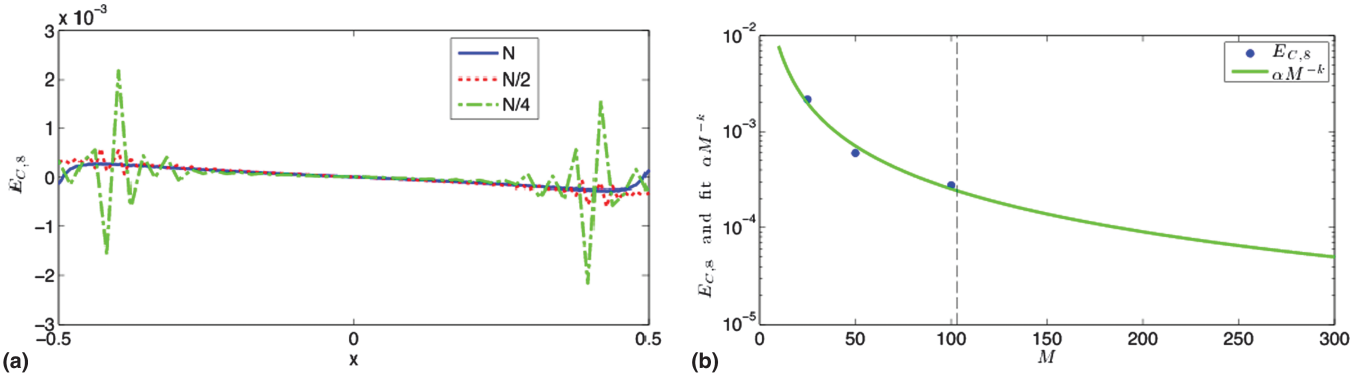

Fig. 10. (a) Errors $E_{C,8}$ of approximation of ImH (x) by $-H[C_8(\mathrm{R}eH)]$ in the example of a finite element model of a DRAM package with N, $N/2$, and $N/4$, where $N = 100$ was used to estimate the smoothness k of the continuation. (b) Norms of the reconstruction errors $\|E_{C,8}\|_\infty$ with N, $N/2$, and $N/4$, where $N = 100$, superimposed with fitted $\|E_F\|_{L^\infty} \sim C \cdot M^{-k}$, k = 1.4884, and $C = 0.2394$.

To show this, we investigate the error E_F of the approximation of a function g that has k continuous derivatives with a first $2M$-mode Fourier series, given in (21). We note that

$$\|E_F\|_{L^\infty} \sim C \cdot M^{-k}, \tag{26}$$

where C depends on b, k, and $g^{(k)}$. The smoothness order k is not given in practice, but it can be estimated by analyzing the reconstruction errors with N, $N/2$, $N/4$,... samples on the original frequency interval, since they produce 2M, $(2M)/2$, $(2M)/4$,.... Fourier coefficients, respectively, used in the approximation. Here we assume that the discretization error E_p due to finite difference approximation of derivatives of ReH and a noise E_d in data are smaller than E_F, and can be neglected. By taking natural logarithm of both sides of (26), we get

$$\ln \|E_F\|_{L^\infty} \sim \ln C - k \ln k, \tag{27}$$

i.e. $\ln \|E_F\|_{L^\infty}$ is a linear function of ln$k$. Using the reconstruction errors for N, $N/2$, and $N/4$, plotted in Fig. 10a, where $N = 100$, and computing their l_∞ errors, we can approximate k and C in the least squares sense using (27), which gives $k = 1.4884$ and $C = 0.2394$. Then we can extrapolate the behavior of $\|E_F\|_{L^\infty}$ for larger M by equation (26) to see how many approximately Fourier coefficients will be needed to get a prescribed accuracy. This is shown in Fig. 10b, where the norms of reconstruction error $E_{C,8}$ with N, $N/2$, and $N/4$ are superimposed with the fit $C \cdot M^{-k}$. The black, dashed vertical line corresponds to $M = 103$ that determines the number of Fourier coefficients used to approximate ImH via continuation of ReH with $N = 100$. As the graph indicates, the error bound due to approximation of a function with a $2M$ Fourier series decays slowly and it is of the order of 10^{-4} even for $N = 300$. Because of this slow decay of the error with M and very limited number of frequency response samples, the method cannot differentiate between the error due to approximation of a function with a truncated Fourier series and causality violations below 5×10^{-4}.

D. Delayed Gaussian Example

Here we use a Gaussian function with a delay employed in [22] to check causality of interconnects through the minimum-phase and all-pass decomposition. The time-domain impulse-response function is modeled by a Gaussian with the center of the peak t_d and standard deviation σ:

$$h(t, t_d) = \exp\left[-\frac{(t, t_d)^2}{2\sigma^2}\right].$$

With $t_d = 0$, the Gaussian function $h(t, 0)$ is even and cannot be causal. As t_d increases, the center of the peak shifts to the right (see Fig. 11) and for $t_d > 3\sigma$, the impulse-response function $h(t, t_d)$ can be gradually made causal by increasing t_d.

The Fourier transform of $h(t, t_d)$ or its corresponding transfer function $H(w, t_d)$ is

$$H(w, t_d) = \exp[-2(\pi w\sigma)^2 - 2i\pi w t_d],$$

a periodic function damped by an exponentially decaying function. We consider two sets of values of the delay t_d. For small $t_d > 3\sigma$, the function $H(w, t_d)$ is noncausal. For larger values $t_d > 3\sigma$, when the delay t_d is big enough, the transfer function $H(w, t_d)$ should be more and more causal.

We fix $\sigma = 1$. In Fig. 12a, we show R$eH(x)$ with a small delay value $t_d = 0.1$ together with a continuation C_8(ReH). Fig. 12b presents I$mH(x)$ as well as its reconstructions $H[C_8(\mathrm{R}eH)]$ and $H[\mathrm{R}eH]$ with and without continuations, respectively. Both approaches have a very large reconstruction error that suggests that the transfer function $H(w, 0.1)$ is not causal, as expected. Varying b does change the

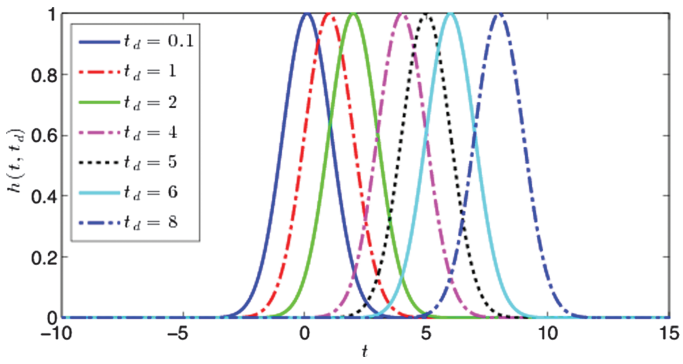

Fig. 11. Impulse-response function $h(t,t_d)$ in the delayed Gaussian example with t_d varying from 0.1 to 8.

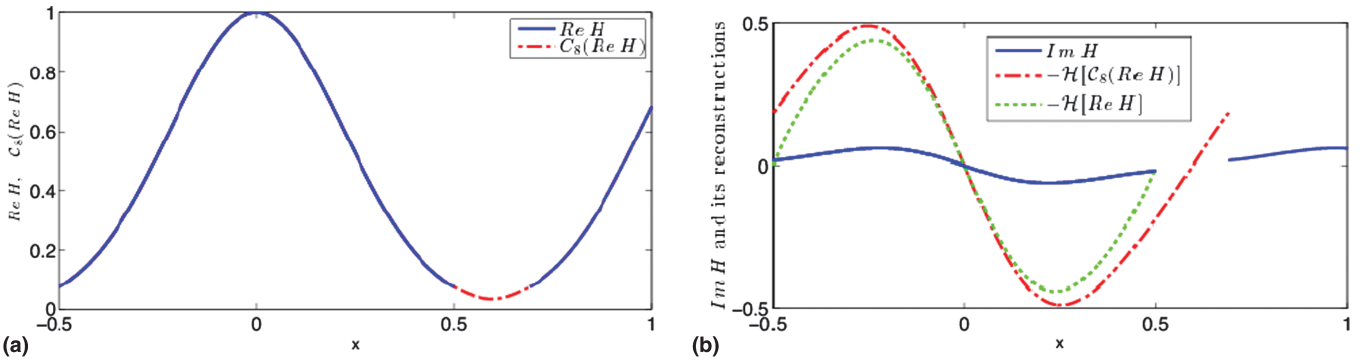

Fig. 12. (a) ReH (x) and C_8 (ReH) in the delayed Gaussian example with $t_d = 0.1$, $N = 1001$, and $b = 0.096$ shown on $[-0.51]$. (b) ImH (x) and its reconstructions $-\mathrm{H}[C_8(\mathrm{R}eH)]$ and $-\mathrm{H}[\mathrm{R}eH]$ with and without continuations, respectively.

actual shape of the error $E_{C,8}$, but does not essentially affect its magnitude.

Next, we set $t_d = 8$ and use the same b to construct the continuation. The results are shown in Fig. 13. Clearly, there is much better agreement between ImH and its reconstructions $-\mathrm{H}[C_8(\mathrm{R}eH)]$ and $-\mathrm{H}[\mathrm{R}eH]$ in both cases, with and without reconstruction.

The reconstruction errors $E_{C,8}$ and E are shown in Fig. 14 and demonstrate the error $E_{C,8}$ with continuation is much smaller than the error E without continuation. The magnitude of $E_{C,8}$ is on the order 2×10^{-4}, about 200 times smaller than E, and it is shown separately in Fig. 14b. In this case, we are able to say that the transfer function $H(w, 8)$ is causal with the error at most 2.5×10^{-4}.

To show gradual change in causality of $H(w, t_d)$, we vary the time delay t_d from 0.1 to 8 and measure l_∞ norms of reconstruction errors $E_{C,8}$ and E. These errors are presented in Table I and shown in Fig. 15. For small values t_d, both errors decrease as t_d increases. For larger t_d, the error $E_{C,8}$ with continuation keeps decreasing until 2.5×10^{-4} with $t_d = 8$, while the error E without continuation saturates at approximately 2.5×10^{-2} starting at $t_d = 1$.

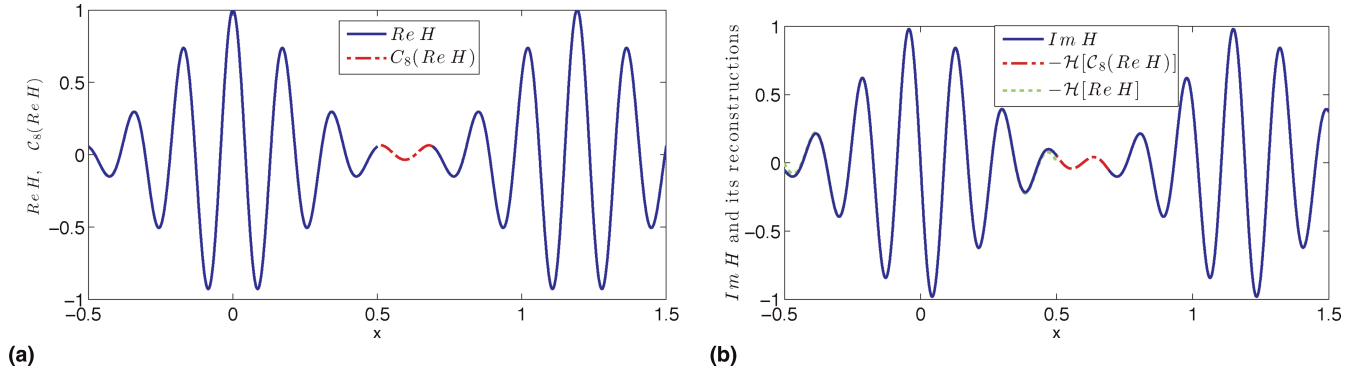

Fig. 13. (a) ReH(x) and C_8(ReH) in the delayed Gaussian example with $t_d = 8$, $N = 1001$, and b = 0.096 shown on $[-0.5, 1.5]$. (b) ImH(x) and its reconstructions $-\mathrm{H}[C_8(\mathrm{R}eH)]$ and $-\mathrm{H}[\mathrm{R}eH]$ with and without continuations, respectively.

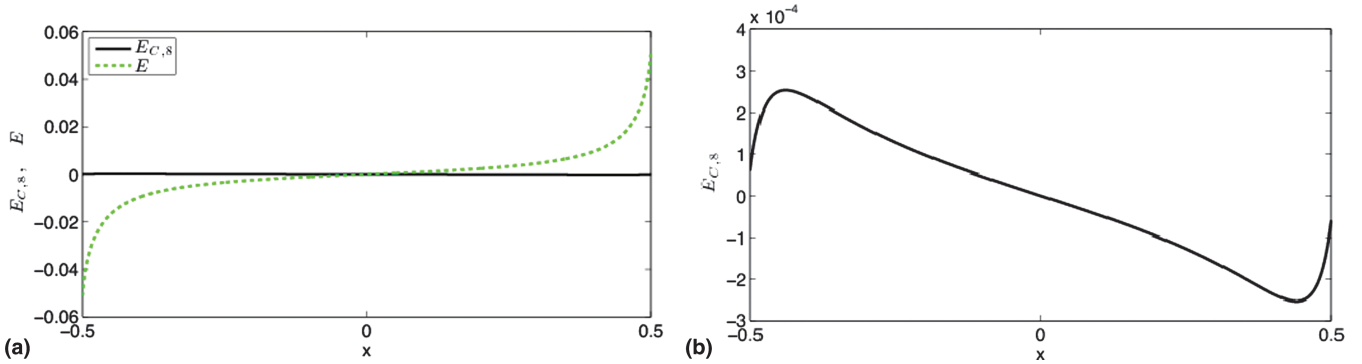

Fig. 14. (a) Error $E_{C,8}$ in the delayed Gaussian example with $N = 1001$, $b = 0.096$ compared with the error E, generated by using Matlab function *hilbert* (without continuation). (b) Zoom-in of the error $E_{C,8}$.

Table I
$\|E_{C,8}\|_\infty$ as t_d Increases Compared With the Corresponding $\|E\|_\infty$ With No Continuation

t_d	$\|E_{C,8}\|_\infty$	$\|E\|_\infty$(no continuation)
0.1	4.2962×10^{-1}	3.8090×10^{-1}
1	8.6566×10^{-2}	5.9440×10^{-2}
2	1.1987×10^{-2}	7.5078×10^{-2}
4	7.1381×10^{-3}	2.8235×10^{-2}
6	3.8170×10^{-3}	6.3803×10^{-2}
8	2.5350×10^{-4}	4.1279×10^{-2}

In the summary, the following algorithm can be used to verify causality of the transfer function $H(w)$ available at a set of equally spaced values $w_j \in [w_{min}, w_{max}], j = 1,\ldots,N$.

- Choose tolerance ε of the causality measure. The developed error estimates could be used as a guidance to determine whether the dominant error comes from the smoothness, accuracy (noise or approximation errors), and resolution of data, or smoothness of a periodic continuation to help in making a decision about causality of the given frequency responses. In practice, ε, for example, could be chosen to coincide with the accuracy of measured or simulated frequency responses.
- With $H(w) = \mathrm{Re}H(w) + i\mathrm{Im}H(w)$ defined on $[w_{min}, w_{max}]$, reflect values of $H(w)$ to $[-w_{max}, -w_{min}]$ using spectrum symmetry of $H(w)$, i.e., ReH and ImH are even and odd functions, respectively.
- Rescale frequency interval to $[-0.5, 0.5]$ by substitution $x = \dfrac{0.5}{w_{max}} w$, if $w_{min} = 0$, to get a function $H(x)$. If $w_{min} > 0$, the rescaled interval is $[-0.5, -a] \cap [a, 0.5]$ with $a = 0.5\dfrac{w_{min}}{w_{max}}$.
- Construct a polynomial continuation $C_m(\mathrm{Re}H)$ of an even degree m using (17), which is a periodic function with the period $1 + 2b$, even, and has continuous derivatives up to the order $m/2$ at $x = \pm 0.5$ if $w_{min} = 0$. For $w_{min} > 0$, use a similar approach to get also a polynomial approximation $\tilde{P}_{m_0}$ defined on $[-a, a]$ using (20). The default values $b = 0.5$ and $m = 8$ are recommended. Higher values of m will provide higher smoothness of the continuation in the extended domain and will allow further decrease in boundary artifacts that are due to mismatch of values of ReH and its derivatives.
- To reconstruct ImH, compute $-\mathrm{H}[C_m(\mathrm{Re}H)]$ spectrally using, for example, FFT/IFFT routines: Calculate the discrete Fourier transform of $C_m(\mathrm{Re}H)$ by FFT and multiply the obtained Fourier coefficients by $isgn(k)$, where k is the wave number. Then apply the inverse discrete Fourier transform to the result via IFFT and multiply it by -1.
- Compute the reconstruction error $E_{C,m}(x)$, $x \in [-0.5, 0.5]$, defined in (18). l_∞ norm, for example, can be used to compare $\|E_{C,m}\|_\infty$ with the given tolerance ε. If $\|E_{C,m}\|_\infty < \varepsilon$, then the function $H(x)$, and, hence, $H(w)$, are causal with the error not exceeding ε. In this case, the method will not be able to differentiate whether the error comes from the lack of resolution or smaller than the tolerance causality violations. Other norms like l_2 norm can be used as well.
- Since an optimal value of b depends on the specific function being approximated, a smaller reconstruction error may be obtained with b other than 0.5. Varying b in small increments with values larger or smaller than the default value $b = 0.5$ may produce a smaller reconstruction error. For smooth functions, a larger value $0.5 < b < 2$ may give better results, while for functions that have high frequency oscillations and steep slopes in the boundary regions, a smaller value $0 < b < 0.5$ may produce smaller reconstruction error. Note that larger values of b may require higher resolution of data.
- If $\|E_{C,m}\|_\infty \geq \varepsilon$, the function $H(x)$, and, hence, $H(w)$, are not causal. For noncausal systems, varying b does not essentially affect the magnitude of the error.

Conclusions

We present a numerical method that can be employed to verify and enforce, if necessary, causality of bandlimited frequency responses before these data are used in macromodeling. The approach is based on dispersion relations and polynomial periodic continuations. Given a transfer function $H(w) = \mathrm{Re}H(w) + i\mathrm{Im}H(w)$, whose discrete values are available on a finite-length frequency interval, the approach constructs a degree m polynomial periodic continuation $C_m(\mathrm{Re}H)$ of ReH by requiring the continuation to be periodic on a wider domain and smooth at the boundary. ImH is reconstructed by computing the minus Hilbert transform of $C_m(\mathrm{Re}H)$ spectrally using FFT/IFFT routines and the result is compared with ImH on the

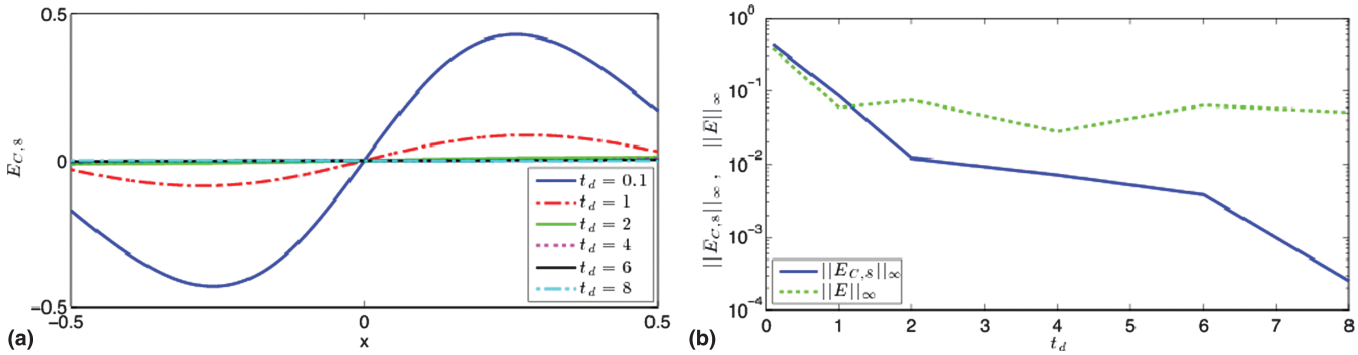

Fig. 15. (a) Error $E_{C,8}$ as t_d varies from 0.1 to 8 in the delayed Gaussian example with $N = 1001$, $b = 0.096$. (b) $\|E_{C,8}\|_\infty$ as a function of t_d compared with $\|E\|_\infty$ (without continuation).

original frequency interval. The approach is able to significantly decrease the boundary artifacts that are due to the lack of out-of-band frequency responses, and are applicable to both baseband and bandpass cases. It is also able to detect small smooth causality violations that are typically difficult to detect in practice. The accuracy of the method and its sensitivity to detect small causality violations primarily depend on the smoothness of the continuation, i.e., the polynomial degree m. The approach eliminates the necessity of approximating the transfer function for large w and does not require truncation of the computational domain to evaluate the Hilbert transform numerically, which is known to be a course of significant boundary errors. In cases when causality is expected, the reconstruction error can be tuned by varying the length of the extended domain. For noncausal systems, increasing m or varying the length of the extended domain does not affect the magnitude of the error.

Acknowledgments

This work was funded by the Micron Foundation. The author L.L.B. would also like to acknowledge the availability of computational resources made possible through the National Science Foundation Major Research Instrumentation Program: grant no. 1229766.

References

[1] M. Swaminathan and E. Engin, *Power Integrity Modeling and Design for Semiconductors and Systems*, Prentice Hall, Upper Saddle River, NJ, 2007.

[2] B. Gustavsen and A. Semlyen, "Rational approximation of frequency domain responses by vector fitting," *IEEE Transactions on Power Delivery*, Vol. 14, No. 3, pp. 1052-1061, 1999.

[3] D. Deschrijver, B. Haegeman, and T. Dhaene, "Orthonormal vector fitting: a robust macromodeling tool for rational approximation of frequency domain responses," IEEE *Transactions on Advanced Packaging*, Vol. 30, No. 2, pp. 216-225, 2007.

[4] P. Triverio, S. Grivet-Talocia, M.S. Nakhla, F.G. Canavero, and R. Achar, "Stability, causality, and passivity in electrical interconnect models," *IEEE Transactions on Advanced Packaging*, Vol. 30, No. 4, pp. 795-808, 2007.

[5] A.V. Oppenheim and R.W. Schafer, *Discrete-Time Signal Processing*," Prentice Hall, Upper Saddle River, NJ, 1989.

[6] W. Cai, D. Gottlieb, and C.-W. Shu, "On one-sided filters for spectral Fourier approximations of discontinuous functions," *SIAM Journal on Numerical Analysis*, Vol. 29, No. 4, pp. 905-916, 1992.

[7] E. Tadmor, "Filters, mollifiers and the computation of the Gibbs phenomenon," *Acta Numerica*, Vol. 16, pp. 305-378, 2007.

[8] H.N. Mhaskar and J. Prestin, "Polynomial operators for spectral approximation of piecewise analytic functions," *Applied and Computational Harmonic Analysis*, Vol. 26, pp. 121-142, 2009.

[9] G. Beylkin and L. Monzón, "Nonlinear inversion of a band-limited Fourier transform," *Applied and Computational Harmonic Analysis*, Vol. 27, pp. 351-366, 2009.

[10] R.D.L. Kronig, "On the theory of dispersion of x-rays," *Journal of the Optical Society of America*, Vol. 12, No. 6, pp. 547-557, 1926.

[11] H.A. Kramers, "La diffusion de la lumiere par les atomes [The diffusion of light by atoms]," Transactions of Volta Centenary Congress, Como, Italy, 2:545–557, 1927.

[12] S. Amari, M. Gimersky, and J. Bornemann, "Imaginary part of antennas admittance from its real part using Bodes integrals," *IEEE Transactions on Antennas and Propagation*, Vol. 43, No. 2, pp. 220-223, 1995.

[13] Tesche, F.M., "On the use of the Hilbert transform for processing measured CW data," *IEEE Transaction on Electromagnetic Compatibility*, 34:259-266, 1992.

[14] M. Wojnowski, G. Sommer, and R. Weigel, "Device characterization techniques based on causal relationships," *IEEE Transactions on Microwave Theory and Techniques*, Vol. 60, No. 7, pp. 2203-2219, 2012.

[15] L. Knockaert and T. Dhaene, "Causality determination and time delay extraction by means of the eigenfunctions of the Hilbert transform," 2008 IEEE Workshop on Signal Propagation on Interconnects, pp. 19–22, Avignon, France, 12-15 May, 2008.

[16] R. Mandrekar and M. Swaminathan, "Delay extraction from frequency domain data for causal macro-modeling of passive networks," 2005 IEEE International Symposium On Circuits And Systems (ISCAS), pp. 5758–5761, Kobe, Japan, 23-26 May, 2005.

[17] R. Mandrekar and M. Swaminathan, "Causality enforcement in transient simulation of passive networks through delay extraction," 9th IEEE Workshop on Signal Propagation on Interconnects, Proceedings, pp. 25–28, Garmisch Partenkirchen, Germany, 10-13 May, 2005.

[18] S.P. Luo and Z.Z. Chen, "Iterative methods for extracting causal time-domain parameters," *IEEE Transactions on Microwave Theory and Techniques*, 53:969-976, 2005.

[19] B. Young, "Bandwidth and density reduction of tabulated data using causality checking," 2010 IEEE Electrical Design of Advanced Packaging and Systems Symposium (EDAPS 2010), pp. 1-4, Singapore, 7-9 December, 2010.

[20] R. Mandrekar, K. Srinivasan, E. Engin, and M. Swaminathan, "Causal transient simulation of passive networks with fast convolution," Proceedings of the 10th IEEE Workshop on Signal Propagation on Interconnects, pp. 61–64, Berlin, Germany, 9-12 May, 2006.

[21] S.N. Lalgudi, K. Srinivasan, G. Casinovi, R. Mandrekar, E. Engin, M. Swaminathan, and Y. Kretchmer, "Causal transient simulation of systems characterized by frequency-domain data in a modified nodal analysis framework," 15th IEEE Topical Meeting on Electrical Performance of Electronic Packaging, pp. 123–126, Scottsdale, AZ, 23-25 Oct, 2006.

[22] B.S. Xu, X.Y. Zeng, J. He, and D.-H. Han, "Checking causality of interconnects through minimum-phase and all-pass decomposition," Proceedings of the 2006 Conference on High Density Microsystem Design and Packaging and Component Failure Analysis (HDP '06), pp. 271–273, 2006.

[23] P. Triverio and S. Grivet-Talocia, "A robust causality verification tool for tabulated frequency data," 10th IEEE Workshop on Signal Propagation on Interconnects, Proceedings, pp. 65–68, Berlin, Germany, 9-12 May, 2006.

[24] P. Triverio and S. Grivet-Talocia, "On Checking Causality of Bandlimited Sampled Frequency Responses," In: Malcovati, P. and Baschirotto, A., eds, PRIME 2006: Proceedings of the 2nd Conference on Ph.D. Research in Microelectronic and Electronics, pp. 501–504, Otranto, Italy, 12-15 June, 2006.

[25] P. Triverio and S. Grivet-Talocia, "Robust causality characterization via generalized dispersion relations," *IEEE Transactions on Advanced Packaging*, Vol. 31, No. 3, pp. 579-593, 2008.

[26] A. Dienstfrey and L. Greengard, "Analytic continuation, singular-value expansions, and Kramers-Kronig analysis," *Inverse Problems*, Vol. 17, No. 5, pp. 1307-1320, 2001.

[27] H.A. Aboutaleb, L.L. Barannyk, A. Elshabini, and F. Barlow, "Causality enforcement of DRAM package models using discrete Hilbert transforms," Proceedings of the 2013 IEEE Workshop on Microelectronics and Electron Devices, pp. 21–24, Boise, ID, 12 April, 2013.

[28] Barannyk, L. L. and Aboutaleb, H. A. and Elshabini, A. and Barlow, F. Spectrally accurate causality enforcement using SVD-based Fourier continuations. Submitted *IEEE Transacations on Components and Packaging Technologies Manufacturing Technology*, ArXiv 1411.3812.

[29] J.W. Cooley and J.W. Tukey, "An algorithm for machine calculation of complex Fourier series," *Mathematics of Computation*, Vol. 19, No. 90, pp. 297-301, 1965.

[30] H.M. Nussenzveig, *Causality and Dispersion Relations*, Academic Press, Waltham, MA, 1972.

[31] H. Dym and H.P. McKean, *Fourier Series and Integrals of Probability and Mathematical Statistics*, Academic Press, Waltham, MA, 1985.

[32] E.J. Beltrami and M.R. Wohlers, *Distributions and the Boundary Values of Analytic Functions*, Academic Press, Waltham, MA, 1966.

[33] M.J. Ablowitz and A.S. Fokas, *Complex Variables: Introduction and Applications of Cambridge Texts in Applied Mathematics*, Cambridge University Press, Cambridge, UK, 1997.

[34] J.P. Boyd, "A comparison of numerical algorithms for Fourier extension of the first, second, and third kinds," *Journal of Computational Physics*, Vol. 178, No. 1, pp. 118-160, 2002.

[35] O.P. Bruno, "Fast, high-order, high-frequency integral methods for computational acoustics and electromagnetics," In: M. Ainsworth, P. Davies,

D. Duncan, P. Martin, and B. Rynne, B., eds, *Topics in Computational Wave Propagation: Direct and Inverse Problems in Lecture Notes In Computational Science and Engineering*, Springer, Berlin, 2003.

[36] O.P. Bruno, Y. Han, and M.M. Pohlman, "Accurate, high-order representation of complex three-dimensional surfaces via Fourier continuation analysis," *Journal of Computational Physics*, Vol. 227, No. 2, pp. 1094-1125, 2007.

[37] M. Lyon, "Approximation error in regularized SVD-based Fourier continuations," *Applied Numerical Mathematics*, Vol. 62, No. 12, pp. 1790-1803, 2012.

[38] M. Lyon, "Sobolev smoothing of SVD-based Fourier continuations," *Applied Mathematics Letters*, Vol. 25, No. 12, pp. 2227-2231, 2012.

[39] M. Lyon and O.P. Bruno, "High-order unconditionally stable FC-AD solvers for general smooth domains II. Elliptic, parabolic and hyperbolic PDEs; theoretical considerations," *Journal of Computational Physics*, Vol. 229, No. 9, pp. 3358-3381, 2010.

[40] B. Bradie, *A Friendly Introduction to Numerical Analysis*," Pearson Prentice Hall, Upper Saddle River, NJ, 2005.

[41] E.W. Cheney, *Introduction to Approximation Theory*, AMS Chelsea Publishing, Providence, RI, 2000.

[42] L.L. Barannyk, H.A. Aboutaleb, A. Elshabini, and F. Barlow, "Causality enforcement of high-speed interconnects via periodic continuations," Proceedings of the 47th International Symposium on Microelectronics, IMAPS 2014, Orlando, FL, 14-16 October, 2014.